Contents lists available at ScienceDirect

J. Chem. Thermodynamics

Self-diffusion coefficients of the binary (H$_2$O + CO$_2$) mixture at high temperatures and pressures

Othonas A. Moultos [a], Ioannis N. Tsimpanogiannis [a,b,*], Athanassios Z. Panagiotopoulos [c], Ioannis G. Economou [a,*]

[a] Chemical Engineering Program, Texas A&M University at Qatar, P.O. Box 23847, Doha, Qatar
[b] Environmental Research Laboratory, National Center for Scientific Research "Demokritos", 15310 Aghia Paraskevi Attikis, Greece
[c] Chemical and Biological Engineering Department, Princeton University, Princeton, NJ 08544, USA

A B S T R A C T

An extensive study of the self-diffusion coefficients in the (H$_2$O + CO$_2$) mixture was carried out using atomistic molecular dynamics simulations. The conditions studied cover a wide range of temperatures (323.15 K $\leqslant$ T $\leqslant$ 1023.15 K) and pressures (200 MPa $\leqslant$ P $\leqslant$ 1000 MPa), of interest for geological and carbon sequestration applications. A combination of simple but accurate point charge force fields was employed, specifically the TIP4P/2005 for H$_2$O and EPM2 for CO$_2$. The simulations were found to be in good agreement with available experimental data at these high temperature and pressure conditions, but extend at conditions for which experiments have not been previously reported. The results were correlated with a generalized form of the Speedy–Angel (1976) relationship. The new phenomenological correlation is a function of pressure and temperature and is shown to reproduce all values to excellent accuracy. Thus, it can be used reliably for engineering calculations.

© 2015 Elsevier Ltd. All rights reserved.

1. Introduction

Accurate knowledge of thermodynamic and transport properties of the (H$_2$O + CO$_2$) mixture is of great importance for a large number of industrial [1], geological [2] and environmental [3] applications. Numerous experimental and theoretical studies have been published, at conditions relevant to enhanced oil recovery [4], CO$_2$ capture and storage (CCS) processes [5], separation equipment design [6], *etc.* Typically, these conditions are in the temperature range of approximately (300 to 600) K and pressures up to 100 MPa.

Diffusion coefficients are among the most important physical properties for this mixture. Mutoru *et al.* [7] presented a comprehensive collection of experimental data up to 2010 of the diffusion coefficient of CO$_2$ in H$_2$O. The majority of 150 experimental data points presented are at pressure of 0.1 MPa. They also reported an empirical methodology for the calculation of the diffusion coefficient at infinite dilution of either of the two components. Magalhaes *et al.* [8] examined the accuracy of a number of

empirical correlations for the diffusion coefficient of CO$_2$ in H$_2$O, using 111 experimental data points, mainly at 0.1 MPa. The experimental data were correlated as a function of temperature and the viscosity or density of the solvent. Additional experimental groups have reported values at temperature below 500 K and pressure below 100 MPa [9–14]. The diffusion coefficient of H$_2$O in CO$_2$ has also been studied for temperatures up to 352 K and pressures up to 30 MPa [15–17].

The (H$_2$O + CO$_2$) mixture can be found in the deep crust [18] and plays an important role in the geochemical evolution of earth. In such depths, the temperature and pressure can be significantly elevated. Wark and Watson [19] reported experimental values for the diffusion of CO$_2$ in H$_2$O at such conditions (759 K $\leqslant$ T $\leqslant$ 961 K, P = 1000 MPa), but the data show considerable scatter and have relative uncertainties of (38 to 66)%. In spite of the geological importance of the mixture, no experimental or simulation values for the diffusion of CO$_2$ in H$_2$O are available for lower pressures in this temperature range, and no values at all for the diffusion of H$_2$O in CO$_2$ in this temperature and pressure range.

Molecular simulation, using accurate atomistic force fields, is an attractive option for the prediction of physical properties of various chemical systems. The primary goal of this work is to use molecular dynamics (MD) simulations to generate self-diffusion coefficients for the (H$_2$O + CO$_2$) mixture at high temperature and

* Corresponding authors at: Chemical Engineering Program, Texas A&M University at Qatar, P.O. Box 23847, Doha, Qatar (I.N. Tsimpanogiannis and I.G. Economou).
E-mail addresses: tsimpano@usc.edu (I.N. Tsimpanogiannis), ioannis.economou @qatar.tamu.edu (I.G. Economou).

pressure conditions (up to 1023 K and 1000 MPa) for which experimental results are scarce, subject to large uncertainties, or altogether lacking. Earlier studies have shown that MD simulation is a valuable tool to complement experimental measurements of transport properties [20,21]. In our recent work [20,22], we showed that the TIP4P/2005 [23] force field in combination with either the EPM2 [24] or TraPPE [25] force fields for CO_2 results in accurate predictions of the diffusion coefficients of H_2O in CO_2 and CO_2 in H_2O. Here, we performed MD simulations using the TIP4P/2005–EPM2 force-field combination. Since earlier studies of this mixture [20,22] were limited to pressures up to 100 MPa and temperatures up to 623 K, the emphasis here was on high temperature and high pressure conditions.

To correlate the new MD simulation results, two different phenomenological models were developed. The first one is based on Arrhenius-type correlations (*e.g.*, Versteeg *et al.* [9], Lu *et al.* [13]), while the second one is rooted to the Speedy–Angell power-law correlation [26]. The resulting expressions provide an accurate correlation of the MD data and because of their computational efficiency they can be a valuable tool for engineering calculations.

This paper is organized as follows: Initially, we report an extensive series of MD simulations for the calculation of self-diffusion coefficients of the ($H_2O + CO_2$) mixture at high pressures and temperatures. Subsequently, these new values are correlated accurately using the phenomenological model based on the generalized Speedy–Angell power-law relationship that is a function of temperature and pressure. The results are also compared against the predictions using the methodology of Mutoru *et al.* [7]. Finally, we end with the conclusions.

2. Molecular dynamics simulations

2.1. Intermolecular potentials

The force fields used for the representation of H_2O and CO_2 molecules were the TIP4P/2005 [23] and EPM2 [27], respectively. The TIP4P/2005 is a rigid 4-site model in which a Lennard–Jones (LJ) sphere is fixed on the oxygen site. The electrostatic contributions are implemented by positive partial charges located on each hydrogen atom and a negative partial charge fixed on an "M-site", located on the bisector of the H—O—H angle at 0.01546 nm from the oxygen atom. The EPM2 force field is a rigid linear 3-site model, with partial charges fixed on the axis of symmetry of the molecule. A negative partial charge is located on the oxygen atom and positive ones on the carbon LJ sites.

The total interactions between molecules i and j, with a total number of m and n sites, respectively, were calculated as the sum of LJ (repulsion + dispersion) interactions and the Coulomb interactions:

$$U_{ij}^{LJ} = \sum_{a=1}^{m}\sum_{b=1}^{n}\left(4\varepsilon_{ij}^{ab}\left[\left(\frac{\sigma_{ij}^{ab}}{r_{ij}^{ab}}\right)^{12} - \left(\frac{\sigma_{ij}^{ab}}{r_{ij}^{ab}}\right)^{6}\right] + \frac{q_i^a q_j^b}{4\pi\varepsilon_0 r_{ij}^{ab}}\right), \qquad (1)$$

where ε_{ij}^{ab} and σ_{ij}^{ab} are the LJ interaction parameters between site a in molecule i and site b in molecule j, respectively, r_{ij}^{ab} is the distance between sites a and b, q_i^a and q_j^b are the charges on site a and b respectively, and ε_0 is the dielectric constant in vacuum. The values of the potential parameters of the force fields used in the present study are listed in table 1.

The LJ parameters for the interaction between atoms belonging to different molecules were calculated using the Lorenz–Berthelot combining rules [28]. An exception was made for the EPM2 model, for which the distance σ_{ij}^{ab} between unlike sites of CO_2 molecules was given by the geometric mean, in accordance with the original

TABLE 1
Force-field parameters for H_2O and CO_2 examined in this study.

TIP4P/2005 [23]		EPM2 [27]	
H—O—H/(°)	104.52	O—C—O/(°)	180
$l_{O–H}$/nm	0.09572	$l_{O–C}$/nm	0.1149
σ_O/nm	0.31589	l_{cq}/nm	0
σ_H/nm	0	σ_C/nm	0.2757
(ε_O/k_B)/K	93.2	σ_O/nm	0.3033
(ε_H/k_B)/K	0	(ε_C/k_B)/K	28.129
q_O/e	−1.1128	(ε_O/k_B)/K	80.507
q_H/e	0.5564	q_C/e	0.6512
		q_O/e	−0.3256

work [27]. Consequently, cross-interaction parameters were calculated from the expressions:

$$\varepsilon_{ij}^{ab} = \left(\varepsilon_i^a \varepsilon_j^b\right)^{\frac{1}{2}}, \qquad (2)$$

$$\sigma_{ij}^{ab} = \begin{cases} \left(\sigma_i^a \sigma_j^b\right)^{\frac{1}{2}} & \text{for} \quad a,b = C_{CO2}, O_{CO2} \text{ for the EPM2 model} \\ \frac{1}{2}\left(\sigma_i^a + \sigma_j^b\right) & \text{otherwise} \end{cases} \qquad (3)$$

2.2. Computational details

All MD simulations were performed in a cubic box with periodic boundary conditions imposed in all directions. The simulation scheme was the following. The system was initially allowed to equilibrate in the (isobaric - isothermal) (*NPT*) ensemble for a period of 2 ns. During this period, the density of the system converged to a mean value, corresponding to the temperature and pressure conditions set. Subsequently, 2 ns production runs were performed in the canonical (*NVT*) ensemble. In both equilibration and production periods, the timestep was 1 fs while the temperature and pressure (only for the equilibration) were maintained constant using the Berendsen [29] method, with the coupling constant of the thermostat set to 0.2 ps and of the barostat to 1 ps. Monitoring of energy, pressure, and temperature during the production period showed that they were well stabilized, with small fluctuations present, typical for any MD simulation. The molecular trajectories were sampled every 2000 steps, resulting in a total of 1000 configurations per simulation, from which all properties of interest were calculated.

Long-range Coulombic interactions were handled using the particle mesh Ewald (PME) method [30,31], which exhibits a faster scaling than the ordinary Ewald summation method [32]. In all the simulations performed, a fourth-order (cubic) interpolation was used along with a Fourier-spacing parameter of 0.12 nm, corresponding to a relative accuracy of approximately $5 \cdot 10^{-3}$ in electrostatic energy calculations. The cut-off distance was set to 1.2 nm, both for the LJ interactions and the PME.

The number of solvent molecules in all production runs was 2000 and the number of solute molecules was 10. This results in a mole fraction for solute equal to $4.98 \cdot 10^{-3}$ which is sufficiently low to make (solute + solute) interactions negligible ("infinite dilution" limit). In addition, this composition is below the solubility limit [33]. More than one solute molecule was used in order to improve the statistics. In order to verify that results are independent of the number of solute molecules in the low composition regime examined, MD simulations with different number of solute molecules (either CO_2 or H_2O) were performed. Details are provided as Supporting Information. In figure S-1, the diffusion coefficient for one, five and ten H_2O molecules in 2000 CO_2 molecules at 750 MPa and $T = (823.15$ and $1023.15)$ K is shown. The diffusion

coefficient of 1, 5 and 10 CO_2 molecules in 2000 H_2O molecules at the same conditions is presented in figure S-2. In all cases, the mean values remain practically unaltered, but the statistical uncertainties decrease from approximately 29% at low solute composition to 9% at high solute composition. These findings are in agreement with previous work for the same mixtures [20].

All the simulations were performed with the open-source package GROMACS [34,35] (Version 4.6.5). Each run was executed in 32 cores, with Intel Xeon 2.7 GHz processors, and needed about 5 wall-clock hours to be completed.

The self-diffusion coefficients, D, were calculated using the Einstein relation, according to which D is obtained from the solute mean square displacement [36]:

$$D = \frac{1}{6} \lim_{t \to \infty} \frac{d}{dt} \left\langle \frac{1}{N} \sum_{i=1}^{N} [\mathbf{r}_i(0) - \mathbf{r}_i(t)]^2 \right\rangle, \qquad (4)$$

where $\mathbf{r}_i(t)$ is the "unfolded" position (which could be outside the central box) of the centers of mass of the solutes at time t, and the angle brackets indicate an ensemble average over all solute molecules and time origins. In order to further improve the statistics of our results, the diffusion coefficient for each state point was calculated from 50 different simulations, each one starting from a different initial configuration, thus leading to a wide divergence of the trajectories of the molecules. We obtained the final results by averaging the diffusion coefficients from the individual runs. The method described above ensured relatively low statistical errors, from approximately (5 to 13)%, that are similar to or lower than those reported in other MD studies in the literature for this mixture [20,21], and lower than the experimental uncertainty of the results of Wark and Watson [19].

As the concentration of the solute increases, the Maxwell–Stefan diffusion coefficient should be used to describe the diffusivity. The Maxwell–Stefan diffusion coefficient of H_2O in CO_2 was studied extensively through MD simulations by Moultos et al. [22]. At the infinite dilution limit, the self- and Maxwell–Stefan diffusion coefficients are identical.

3. Results and discussion

Initially, the two force fields, TIP4P/2005 and EPM2, were evaluated for the prediction of the density of the two pure components at high temperatures and pressures. In figure 1, experimental values [37] and *NPT* MD predictions are shown for H_2O density (top) and for CO_2 density (bottom). Tabulated values are provided in Supporting Information (tables S-1 and S-2). The percentage deviation between experimental data for H_2O and TIP4P/2005 predictions is in the range (0.1 to 1.4)%; thus the TIP4P/2005 model describes well the density of H_2O. For the case of CO_2, the deviation between experimental data and EPM2 predictions is larger and varies between (1 and 4)%. Overall, the accuracy of both force fields is considered to be very good.

Analysis of the diffusion coefficient calculations is initially performed for CO_2 in H_2O at 1000 MPa and different temperatures, since it corresponds to the only set of available experimental values [19]. As shown in figure 2, agreement between experimental values and simulations is good, within or near the uncertainty limits in the experimental results. The simulation results, however, are much less scattered than the experimental values at the higher temperatures. Thus, when also taking into account the excellent agreement with experimental values at lower temperatures and pressures obtained earlier [20,22], one can expect that the force field would be reasonably accurate in the other conditions examined, of pressures between (250 and 1000) MPa, and temperatures between (323.15 and 1023.15) K.
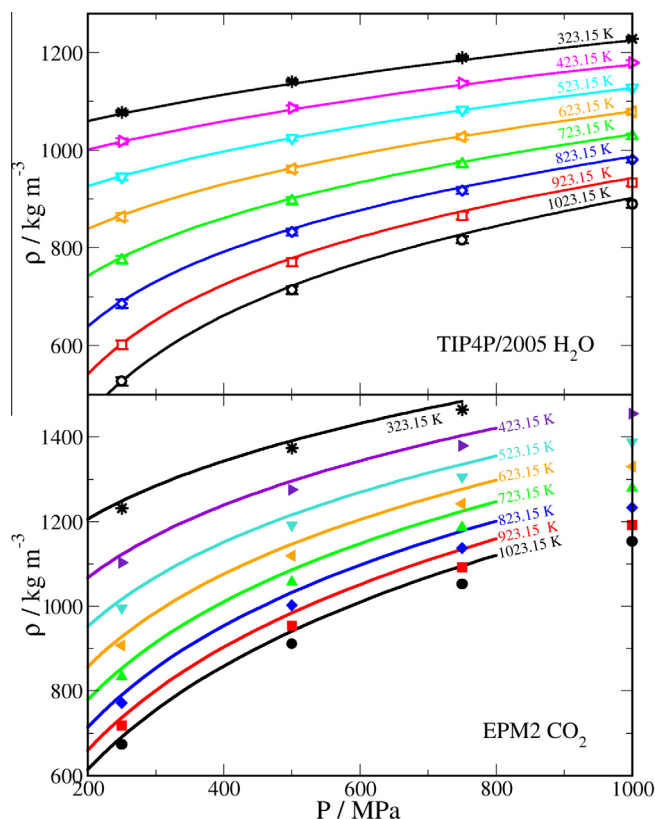

FIGURE 1. Experimental data (lines [37]) and MD predictions (points) for the density of TIP4P/2005 H_2O (top) and EPM2 CO_2 (bottom).
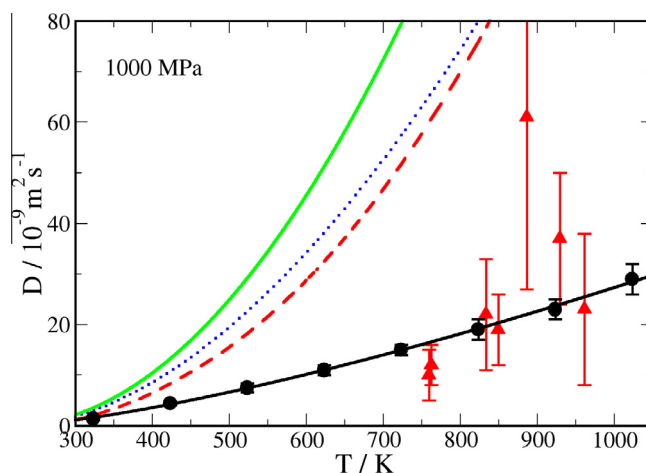

FIGURE 2. Diffusion coefficient of CO_2 in H_2O as a function of temperature at 1000 MPa. Experimental data by Wark and Watson [19] (red triangles), MD simulations (black circles) and correlations (lines). The black solid line denotes calculations with the new correlation (equations (7)–(9)). The dotted blue line denotes calculations with the correlation of Moultos et al. [20]. Green solid line denotes calculations with the correlation of Zeebe [21]. Red dashed line denotes calculations at 1000 MPa using the methodology of Mutoru et al. [7]. (For interpretation of the references to colour in this figure legend, the reader is referred to the web version of this article.)

In figure 3, the diffusion coefficient of CO_2 in H_2O at different temperatures and pressures from the MD simulations is shown. Tabulated values are reported in table S-1 of the Supporting Information. No experimental results are available at these conditions, other than those already shown in figure 2. The effect of
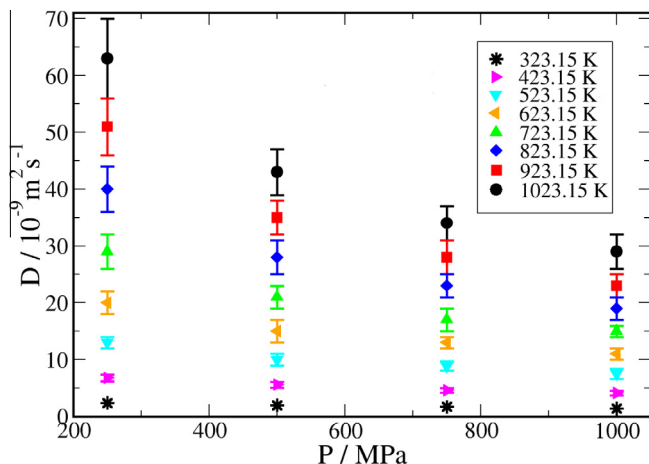
FIGURE 3. MD data for the diffusion coefficient of CO_2 in H_2O as a function of pressure for various temperatures.

FIGURE 5. MD data for the diffusion coefficient of CO_2 in H_2O as a function of temperature for various pressures. Black symbols denote the MD results of the current study. Blue, red and green symbols denote the MD results reported by Moultos et al. [20]. Black lines denote the calculations with the new correlation (equations (7)–(9)). The blue, red and green lines denote calculations with the new correlation at extrapolation conditions. (For interpretation of the references to colour in this figure legend, the reader is referred to the web version of this article.)

pressure on the diffusion coefficient becomes more pronounced as temperature increases.

MD simulation results for the diffusion coefficient of H_2O in CO_2 at the same conditions are presented in figure 4 and table S-2 of the Supporting Information. Overall, the temperature and pressure effect is qualitative similar for both sets of results. Nevertheless, for a given temperature and pressure value, the diffusion coefficient of H_2O in CO_2 is higher than this of CO_2 in H_2O, despite the higher density of CO_2 compared to H_2O at the same conditions.

Although MD simulation is a very reliable approach to predict transport properties, it is fairly time consuming and thus simple empirical correlations of the data are highly desirable. Here, we considered two literature functional relationships, for both the diffusion coefficient of CO_2 in H_2O and H_2O in CO_2 at high pressure and temperature. These two correlations have been used in a number of studies to correlate experimental data [9,13] or molecular simulation results [20,21].

Lu and co-workers [13] used a modified Arrhenius-type of equation, known as the Vogel–Tamann–Fulcher equation in order to correlate their experimental results for the diffusion coefficient of CO_2 in H_2O. These values were in the pressure range (10 to 45) MPa and temperature range (268 to 473) K. The Vogel–Tamann–Fulcher equation reads:
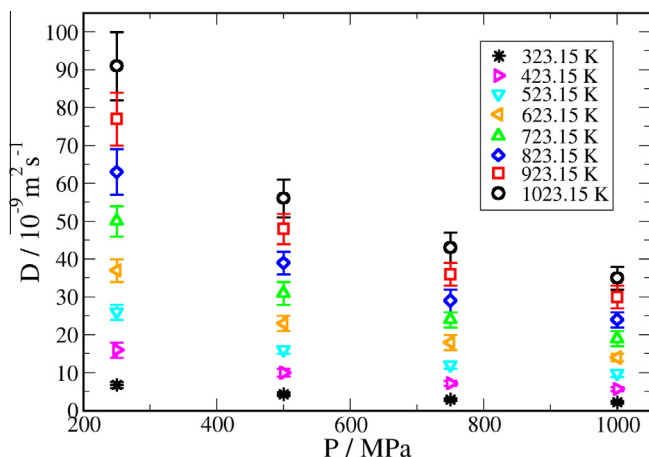

FIGURE 4. MD data for the coefficient of H_2O in CO_2 as a function of pressure for various temperatures.
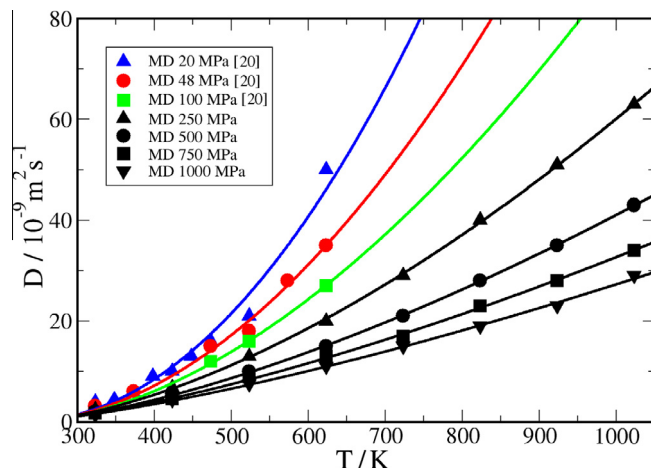
$$D_{CO_2}^{VTF} = \exp\left[\frac{-\alpha}{(T-\beta)} - \gamma\right], \tag{5}$$

where α, β, γ are fitted parameters.

Lu et al. [13] correlated their experimental values more precisely by using a power-law-type equation expressed as:

$$D_{CO_2}^{SA} = D_0\left(\frac{T}{T_s} - 1\right)^m, \tag{6}$$

where D_0, T_s and m are fitted constant parameters. In most cases, T_s = 227 K. This correlation is known as the Speedy–Angell power-law equation [26] and is denoted as SA.

While both type of correlations can describe accurately our MD simulation results when examined at isobaric conditions, we observed that it was not easy to obtain generalized expressions for the parameters for the case of the Vogel–Tamann–Fulcher equation. Therefore, for the remainder of the study we focus our discussion on the SA-type correlation. In particular, we use the following generalized form of the Speedy–Angell equation in order to correlate the MD simulations reported here:

$$D_{solute}^{SA} = D_0(P)\left(\frac{T}{T_s} - 1\right)^{m(P)}, \tag{7}$$

where the subscript solute denotes either CO_2 or H_2O, T_s = 227 K and the parameters D_0 and m are given as functions of pressure P.

In order to correlate the MD results using equation (7), the following procedure was implemented. Initially, the MD simulations were plotted as a function of temperature. For each pressure a set of optimum values for the parameters, D_0 and m, were calculated. Subsequently, the resulting optimum parameters were correlated using the pressure as the primary variable.

For the case of the diffusion coefficient of CO_2 in H_2O, it is:

$$D_0 = a_1 \ln(P/\text{MPa}) + a_2, \tag{8}$$

$$m = b_1 \ln(P/\text{MPa}) + b_2, \tag{9}$$

with: $a_1 = -2.3097 \cdot 10^{-9}$, $a_2 = 2.1064 \cdot 10^{-8}$, $b_1 = -0.17812$, and $b_2 = 2.59406$.

In figure 5, MD simulation data and calculations from equations (7)–(9) are presented. In all cases, the agreement is very good.
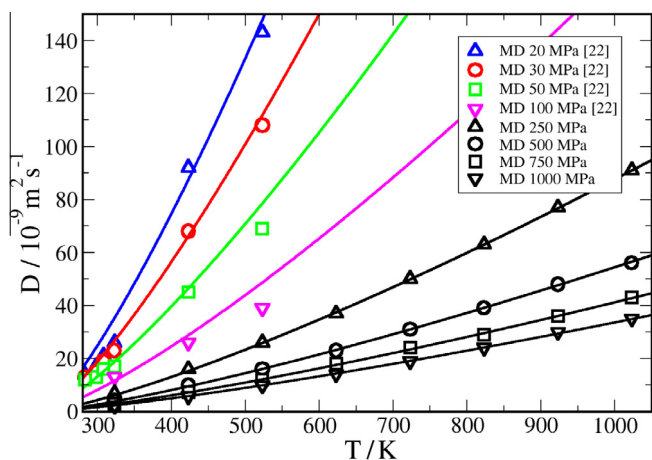
FIGURE 6. MD data for the diffusion coefficient of H_2O in CO_2 as a function of temperature for various pressures. Black symbols denote the MD results of the current study. Blue, red, green and magenta symbols denote the MD results reported by Moultos *et al.* [22]. Black lines denote calculations with the new correlation (equations (7), (10) and (11)) at conditions within the range of development of the correlations. Blue, red, green and magenta lines denote calculations with the new correlation at extrapolation conditions. (For interpretation of the references to colour in this figure legend, the reader is referred to the web version of this article.)

The % Average Absolute Deviation (*AAD*) for the four isobars (250, 500, 750 and 1000 MPa) is 2.6%.

In order to examine the quality of the correlation at other conditions, we calculated the diffusion coefficient of CO_2 in H_2O as a function of temperature at (20, 48, and 100) MPa. The calculated values are compared to the MD simulations, at lower pressures, reported by Moultos *et al.* [20]. Very good agreement was obtained and the % *AAD* was equal to 12.8%.

In figure 2 one can see the comparison of the calculations using four different models with the only available experimental values at high pressures (1000 MPa) reported by Wark and Watson [19]. Note that the MD-based correlations reported by Zeebe [21], and Moultos *et al.* [20] correspond to a temperature and pressure range where the diffusion coefficients of CO_2 in H_2O are independent of pressure. Therefore, significant deviation of these two models from the experimental results at high pressure is expected. Although, the methodology by Mutoru *et al.* [7] takes into account the effect of pressure, the strong deviation from the experimental values is a result of the fact that the methodology included only a very limited amount of data at pressures higher than 0.1 MPa. Therefore, at high pressure conditions, the correlation developed in this work should be preferred.

A similar approach was followed for the case of calculating the diffusion coefficient of CO_2 in H_2O. In this case, the pressure effect on D_0 is described according to the expression:

$$D_0 = a_1(P/\text{MPa})^{a_2}, \tag{10}$$

with: $a_1 = 8.3356 \cdot 10^{-7}$, and $a_2 = -6.8962 \cdot 10^{-1}$, while m is constant:

$$m = 1.27. \tag{11}$$

In figure 6, MD simulation data and correlation calculations are shown. The agreement is excellent and the % *AAD* is equal to 2.0%. The correlation was applied at lower pressures of 20, 30, 50 and 100 MPa and compared against the MD simulations by Moultos *et al.* [22]. Once again, reasonable agreement is observed with the % *AAD* equal to 28.6%. The relatively higher % *AAD* is primarily due to the relatively poorer agreement for the case of 20 MPa.

4. Conclusions

The study of self-diffusion coefficients of ($H_2O + CO_2$) at high temperature and pressure conditions is of crucial importance for understanding the geological evolution of earth since this binary mixture can be found in the deep earth crust. In this study, MD simulations were performed, using the relatively simple but accurate TIP4P/2005 for H_2O and EPM2 for CO_2 force fields for the calculation of these diffusion coefficients, at a very wide range of conditions (323.15 K $\leqslant$ T $\leqslant$ 1023.15 K, and 200 MPa $\leqslant$ P $\leqslant$ 1000 MPa). For such conditions, very few experimental or simulation values are available in the open literature. The simulations results were found to be in very good agreement with a single experimental data set at 1000 MPa for the self-diffusion coefficient of CO_2 in H_2O. In the current study, we also reported density MD values that are in good agreement with experimental values. Furthermore, a simple and computationally efficient phenomenological model was developed that predicts the self-diffusion coefficients as a function of pressure and temperature. The proposed model is in the form of a generalized Speedy–Angel correlation. The proposed correlations provide high accuracy and are simple to use.

Acknowledgements

Appendix A. Supplementary data

Supplementary data associated with this article can be found, in the online version, at http://dx.doi.org/10.1016/j.jct.2015.04.007.

References

[1] X. Liu, A. Martín-Calvo, E. McGarrity, S.K. Schnell, S. Calero, J.M. Simon, D. Bedeaux, S. Kjelstrup, A. Bardow, T.J.H. Vlugt, Ind. Eng. Chem. Res. 51 (2012) 10247–10258.
[2] L.M. Hamm, I.C. Bourg, A.F. Wallace, B. Rotenberg, Rev. Mineral. Geochem. 77 (2013) 189–228.
[3] P.B. Bedient, H.S. Rifai, C.J. Newell, Ground Water Contamination: Transport and Remediation, Prentice-Hall: Englewood Cliffs, NJ, USA, 1994.
[4] C.M. Oldenburg, K. Pruess, S.M. Benson, Energy Fuels 15 (2001) 293–298.
[5] B. Metz, O. Davidson, H. de Coninck, M. Loos, L. Meyer, Carbon Dioxide Capture and Storage: Special Report of the Intergovernmental Panel on Climate Change, Cambridge University Press, 2005.
[6] B. Rumpf, H. Nicolaisen, C. Öcal, G. Maurer, J. Solution Chem. 23 (1994) 431–448.
[7] J.W. Mutoru, A. Leahy-Dios, A. Firoozabadi, AIChE J. 57 (2011) 1617–1627.
[8] A.L. Magalhães, P.F. Lito, F.A. Da Silva, C.M. Silva, J. Supercrit. Fluids 76 (2013) 94–114.
[9] G.F. Versteeg, W. Van Swaalj, J. Chem. Eng. Data 33 (1988) 29–34.
[10] M.J. Frank, J.A. Kuipers, W.P. van Swaaij, J. Chem. Eng. Data 41 (1996) 297–302.
[11] S.O.K. Hirai, H. Yazawa, H. Ito, Y. Tabe, K. Hijicata, Energy 22 (1997) 363–367.
[12] F. Tewes, F. Boury, J. Phys. Chem. B 109 (2005) 3990–3997.
[13] W. Lu, H. Guo, I.M. Chou, R.C. Burruss, L. Li, Geochim. Cosmochim. Acta 115 (2013) 183–204.
[14] S.P. Cadogan, G.C. Maitland, J.P.M. Trusler, J. Chem. Eng. Data 59 (2014) 519–525.
[15] B. Xu, K. Nagashima, J.M. DeSimone, C.S. Johnson, J. Phys. Chem. A 107 (2002) 1–3.
[16] D.N. Espinoza, J.C. Santamarina, Water Resour. Res. 46 (2010) 7537 (07531–07510).
[17] F.A. Schwertz, J.E. Brow, J. Chem. Phys. 19 (1951) 640–646.
[18] J. Walther, P. Orville, Contrib. Mineral. Petrol. 79 (1982) 252–257.
[19] D.A. Wark, E.B. Watson, Geochim. Cosmochim. Acta 68 (2004) 2693–2698.
[20] O.A. Moultos, I.N. Tsimpanogiannis, A.Z. Panagiotopoulos, I.G. Economou, J. Phys. Chem. B 118 (2014) 5532–5541.

[21] R.E. Zeebe, Geochim. Cosmochim. Acta 75 (2011) 2483–2498.
[22] O.A. Moultos, G.A. Orozco, I.N. Tsimpanogiannis, A.Z. Panagiotopoulos, I.G. Economou, Mol. Phys. (in press). http://dx.doi.org/10.1080/00268976.2015.1023224.
[23] J.L.F. Abascal, C. Vega, J. Chem. Phys. 123 (2005) 234505–234512.
[24] J.G. Harris, K.H. Yung, J. Phys. Chem. 99 (1995) 12021–12024.
[25] J.J. Potoff, J.I. Siepmann, AIChE J. 47 (2001) 1676–1682.
[26] R.J. Speedy, C.A. Angell, J. Chem. Phys. 65 (1976) 851–858.
[27] J. Harris, K. Yung, J. Phys. Chem. 99 (1995) 12021.
[28] M.P. Allen, D.J. Tildesley, Computer Simulation of Liquids, Oxford University Press, 1987.
[29] H.J.C. Berendsen, J.P.M. Postma, W.F. van Gunsteren, A. DiNola, J.R. Haak, J. Chem. Phys. 81 (1984) 3684–3690.
[30] T. Darden, D. York, L. Pedersen, J. Chem. Phys. 98 (1993) 10089–10092.
[31] U. Essmann, L. Perera, M.L. Berkowitz, T. Darden, H. Lee, L.G. Pedersen, J. Chem. Phys. 103 (1995) 8577–8593.
[32] P.P. Ewald, Ann. Phys. 64 (1921) 253–287.
[33] Y. Liu, A.Z. Panagiotopoulos, P.G. Debenedetti, J. Phys. Chem. B 115 (2011) 6629–6635.
[34] H.J.C. Berendsen, D. van der Spoel, R. van Drunen, Comput. Phys. Commun. 91 (1995) 43–56.
[35] E. Lindahl, B. Hess, D. van der Spoel, J. Mol. Model. 7 (2001) 306–317.
[36] A. Einstein, Ann. Phys. 17 (1905) 549–560.
[37] E.W. Lemmon, M.O. McLinden, D.G. Friend, P.J. Linstrom, W.G. Mallard, NIST Chemistry WebBook 2014.

JCT 15-99